HETEROCYCLES, Vol. 98, No. 2, 2019, pp. 224 - 235. © 2019 The Japan Institute of Heterocyclic Chemistry
Received, 15th December, 2018, Accepted, 18th January, 2019, Published online, 7th February, 2019
DOI: 10.3987/COM-18-14024

SYNTHESIS, CRYSTAL STRUCTURE, SPECTROSCOPIC AND COMPUTATIONAL STUDIES OF 2-{1-[2-(1,3-DIMETHYL-4-NITRO-1*H*-PYRAZOL-5-YL)HYDRAZONO]ETHYL}PYRIDINE

Ahmad S. Abushamleh,[1]* Kayed A. Abu-Safieh,[1]* Monther A. Khanfar,[2] Khaleel I. Assaf,[3] Bader A. Salameh,[1] and Nisreen J. Alwahsh[1]

[1]Department of Chemistry, Faculty of Science, Hashemite University, P.O. Box 330127, Zarqa 13133, Jordan. [2]Department of Chemistry, The University of Jordan, Amman 11942, Jordan. [3]Department of Chemistry, Faculty of Science, Al-Balqa Applied University, P.O. Box 19117, Al-Salt, Jordan. E-mail: shamleh@hu.edu.jo, kayedas@hu.edu.jo

Abstract – 2-{1-[2-(1,3-Dimethyl-4-nitro-1*H*-pyrazol-5-yl)hydrazono]ethyl}-pyridine has been prepared from 5-hydrazino-1,3-dimethyl-4-nitro-1*H*-pyrazole and 2-acetylpyridine in an ethanolic solution. It crystallizes as an (*E*/*Z*) isomeric pair in the triclinic space group P-1 with the lattice parameters: a = 10.357(1) Å, b = 11.613(1) Å, c = 13.069(1) Å, α = 67.74(1)°, β = 70.77(1)°, γ = 67.92(1)°, volume = 1315.6(3) Å^3, Z = 2. The isomeric pair (*E*/*Z*) is contained in the unit cell, where the N-H group is H-bonded to the pyridine nitrogen and to the oxygen of the nitro group in the *Z*-isomer and to the oxygen of the nitro group only in the *E*-isomer. NMR showed that the *E*-isomer is the major. DFT calculations were performed to further investigate the electronic properties of the synthesized compound.

INTRODUCTION

Hydrazones and their metal chelates constitute an important class of compounds which have many pharmacological applications such as antimicrobial, anticonvulsant, anti-inflammatory, and anticancer agents.[1-4] 2-Acetylpyridine and 2-benzoylpyridine-derived hydrazones and their metal complexes have shown significant antiproliferative and cytotoxic activities.[5,6] Pyrazole, the central core in pyrazole derivatives, is a five-membered heterocyclic organic compound with two adjacent nitrogen atoms. Many derivatives of pyrazole have been utilized in a wide range of agricultural, pharmaceutical, and chemical

industries.[7] In particular, pyrazole derivatives are known to possess a wide range of biological activities such as their capabilities of being antimicrobial, antifungal, antitubercular, anti-inflammatory, anticonvulsant, antitumor, and antiviral agents.[8-15] The title compound 2-{1-[2-(1,3-dimethyl-4-nitro-1*H*-pyrazol-5-yl)hydrazono]ethyl}pyridine (**4**, Scheme 1) was originally prepared as a potential bidentate Schiff-base ligand by reacting 1,3-dimethyl-4-nitro-5-chloropyrazole (**1**) with hydrazine hydrate followed by reaction with 2-acetylpyridine. The coordination chemistry of the ligand system exemplified by **4** with transition metals is underway. However, because of some difficulties experienced in this direction, we decided to study the structural properties of **4** and we therefore, report the synthesis and structural characterization of the new hydrazone **4**. The electronic structure of **4** has also been characterized by using density functional theory (DFT).

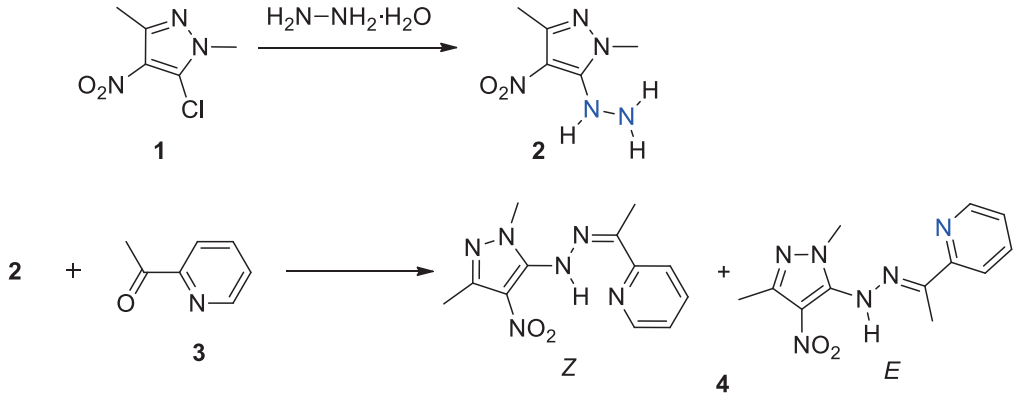

Scheme 1. The synthetic steps for the preparation of **4**

RESULTS AND DISCUSSION

The reaction of 5-hydrazino-1,3-dimethyl-4-nitro-1*H*-pyrazole, (**2**) with acetylpyridine, (**3**) in boiling absolute ethanol and in equimolar ratio gives the hydrazone Schiff base ligand (**4**) in excellent yield (Scheme 1). ^{1}H NMR, and ^{13}C NMR, and IR spectral data support the formula assignments. The IR spectrum of **4** shows appearance of a strong band in the region 1614-1622 cm^{-1} assignable to the ν(C=N) imine group.[16,17] Obviously, the hydrazones resulting from 2-acetylpyridine and hydrazines should, in principle, give rise to an *E*/*Z* type of isomerism. It has been noticed that all the signals of ^{1}H NMR spectra were duplicated showing the two *E*- and *Z*-isomers in which the *E*-isomer was the major. The N-H signal for the *Z*-isomer was resonated at 15.80 ppm, while the *E*-isomer showed this signal at 10.23 ppm indicating the H-bonding behavior with the nitrogen atom of the pyridine ring and the oxygen atom of the nitro group in the Z-isomer (minor). This isomerism was confirmed by single crystal X-ray structural determination of **4**.

X-RAY STRUCTURAL RESULTS

The original aim of the work was to prepare compound **4** (Scheme 1) for the purpose of exploring its capacity as a bidentate chelate ligand, utilizing the pyridine nitrogen and the azo-nitrogen being suitably situated for coordination to transition metals. The difficulties that we encountered in this direction necessitate the study of the X-ray structural properties of **4**. It is worth noting that numerous literature reports have described hydrazones derived from 2-acetylpyridine and hydrazine derivatives and in many cases the subsequent complexation of these with metal cations.[18-20] Surprisingly, in very few cases the probability of (*E*/*Z*) isomerism on the part of the hydrazones was studied.[5,6] However, single crystal X-ray structural determination of **4** revealed the presence of this type of isomerism. Figure 1 shows the two isomers *E* and *Z* in the unit cell. In both isomers the structural fragment, consisting of the pyrazole ring and the N-H group, is in the same position and the N-H is H-bonded to the same oxygen of the nitro group of the pyrazole ring. With respect to the C=N double bond, the methyl group and the pyridine ring exchange positions in the two isomers. In the *Z*-isomer the pyridine nitrogen is in a position which allows intramolecular H-bonding with the N-H, and in the *E*-isomer these are anti to each other. Clearly, the *Z*-isomer is having the pyridine nitrogen and the imine-nitrogen in a suitable position for coordination to metals. The crystal data are listed in Table 1, bond lengths and angles for both isomers are described in Figure 1 and Tables 2, 3 and they are essentially the same for both isomers.

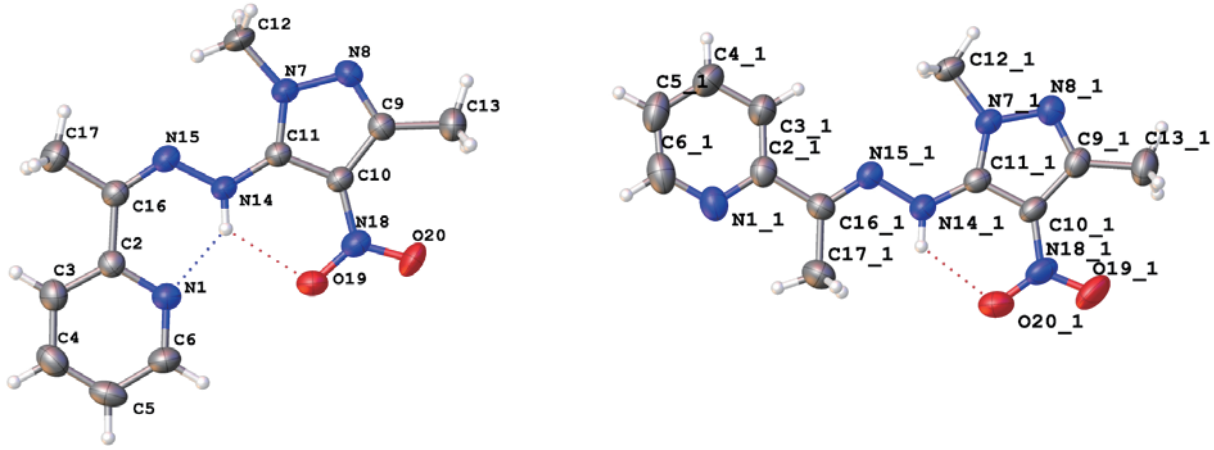

Figure 1. The molecular structure of **4** (*Z*-isomer left and *E*-isomer right), both isomers appear in the unit cell

Table 1. Crystal data and structure refinement for **4**

Empirical formula	$C_{24}H_{28}N_{12}O_4$
Formula weight	548.58
Temperature/K	291
Crystal system	triclinic
Space group	P-1
a/Å	10.357(1)
b/Å	11.613(1)
c/Å	13.069(1)
α/°	67.74(1)
β/°	70.77(1)
γ/°	67.92(1)
Volume/Å^3	1315.6(3)
Z	2
ϱ_{calc}g/cm^3	1.385
μ/mm^{-1}	0.100
F(000)	576.0
Crystal size/mm^3	0.04 × 0.04 × 0.01
Radiation	MoKα (λ = 0.71073)
2θ range for data collection/°	5.962 to 58.872
Index ranges	-13 ≤ h ≤ 14, -15 ≤ k ≤ 15, -16 ≤ l ≤ 17
Reflections collected	11250
Independent reflections	6078 [R_{int} = 0.0296, R_{sigma} = 0.0633]
Data/restraints/parameters	6078/0/368
Goodness-of-fit on F^2	1.029
Final R indexes [I>=2σ (I)]	R_1 = 0.0543, wR_2 = 0.1232
Final R indexes [all data]	R_1 = 0.1081, wR_2 = 0.1510
Largest diff. peak/hole/e Å^{-3}	0.22/-0.20

Table 2. Bond Lengths for **4**

Atom	Atom	Length/Å	Atom	Atom	Length/Å
N1	C2	1.346(3)	N1_1	C2_1	1.332(3)
N1	C6	1.338(3)	N1_1	C6_1	1.347(3)
C2	C3	1.393(3)	C2_1	C3_1	1.372(3)
C2	C16	1.483(3)	C2_1	C16_1	1.491(3)
C3	C4	1.376(3)	C3_1	C4_1	1.373(3)
C4	C5	1.361(3)	C4_1	C5_1	1.371(4)
C5	C6	1.382(3)	C5_1	C6_1	1.374(4)
N7	N8	1.390(2)	N7_1	N8_1	1.405(2)
N7	C11	1.345(2)	N7_1	C11_1	1.325(3)
N7	C12	1.459(3)	N7_1	C12_1	1.458(3)
N8	C9	1.313(3)	N8_1	C9_1	1.303(3)
C9	C10	1.416(3)	C9_1	C10_1	1.430(3)
C9	C13	1.492(3)	C9_1	C13_1	1.495(3)
C10	C11	1.404(3)	C10_1	C11_1	1.394(3)
C10	N18	1.395(3)	C10_1	N18_1	1.384(3)
C11	N14	1.347(2)	C11_1	N14_1	1.351(3)
O20	N18	1.233(2)	N14_1	N15_1	1.374(2)
N14	N15	1.365(2)	N15_1	C16_1	1.289(3)
O19	N18	1.243(2)	C16_1	C17_1	1.504(3)
C17	C16	1.496(3)	N18_1	O19_1	1.233(2)
C16	N15	1.298(2)	N18_1	O20_1	1.250(2)

Table 3. Bond Angles for **4**

Atom	Atom	Atom	Angle/°	Atom	Atom	Atom	Angle/°
C6	N1	C2	119.1(2)	C6_1	N1_1	C2_1	117.4(2)
C3	C2	N1	120.6(2)	C3_1	C2_1	N1_1	122.4(2)
C16	C2	N1	118.0(2)	C16_1	C2_1	N1_1	115.9(2)
C16	C2	C3	121.5(2)	C16_1	C2_1	C3_1	121.7(2)
C4	C3	C2	119.4(2)	C4_1	C3_1	C2_1	119.3(2)

C5	C4	C3	120.0(2)	C5_1	C4_1	C3_1	119.6(3)
C6	C5	C4	118.4(2)	C6_1	C5_1	C4_1	117.7(3)
C5	C6	N1	122.7(2)	C5_1	C6_1	N1_1	123.6(2)
C11	N7	N8	111.3(2)	C11_1	N7_1	N8_1	111.3(2)
C12	N7	N8	116.4(2)	C12_1	N7_1	N8_1	116.5(2)
C12	N7	C11	132.3(2)	C12_1	N7_1	C11_1	132.3(2)
C9	N8	N7	106. 7(2)	C9_1	N8_1	N7_1	106.6(2)
C10	C9	N8	109.9(2)	C10_1	C9_1	N8_1	109.5(2)
C13	C9	N8	120.3(2)	C13_1	C9_1	N8_1	120.6(2)
C13	C9	C10	129.8(2)	C13_1	C9_1	C10_1	129.9(2)
C11	C10	C9	106.2(2)	C11_1	C10_1	C9_1	106.1(2)
N18	C10	C9	127.9(2)	N18_1	C10_1	C9_1	128.7(2)
N18	C10	C11	125.8(2)	N18_1	C10_1	C11_1	125.2(2)
C10	C11	N7	105.9(2)	C10_1	C11_1	N7_1	106.6(2)
N14	C11	N7	127.9(2)	N14_1	C11_1	N7_1	127.3(2)
N14	C11	C10	126.2(2)	N14_1	C11_1	C10_1	126.1(2)
N15	N14	C11	121.4(2)	N15_1	N14_1	C11_1	122.6(2)
O20	N18	C10	119.7(2)	C16_1	N15_1	N14_1	116.2(2)
O19	N18	C10	118.3(2)	N15_1	C16_1	C2_1	116.1(2)
O19	N18	O20	122.0(2)	C17_1	C16_1	C2_1	119.3(2)
C17	C16	C2	118.6(2)	C17_1	C16_1	N15_1	124.6(2)
N15	C16	C2	127.2(2)	O19_1	N18_1	C10_1	120.0(2)
N15	C16	C17	114.2(2)	O20_1	N18_1	C10_1	118.5(2)
C16	N15	N14	119.0(2)	O20_1	N18_1	O19_1	121.4(2)

DFT-calculations

Quantum-chemical calculations were performed to investigate the molecular geometry and the electronic properties of compound **4**. Density functional theory (DFT) was employed using the B3LYP method and 6-311++G** basis set. The optimized structure of the two rotameric isomers in gas phase is shown in Figure 2. *E*-isomer involved the formation of an intramolecular hydrogen bond between the amino group and an oxygen atom on the nitro group (–N–H----O–N–) with a bond distance of 1.96 Å, while *Z*-isomer showed the formation of two intramolecular hydrogen bonds, in which the first hydrogen bond is similar

to that found in *E*-isomer and additional one involved the amino group (–N–H) and the nitrogen atom on the pyridine ring with a short bond distance of 1.85 Å.

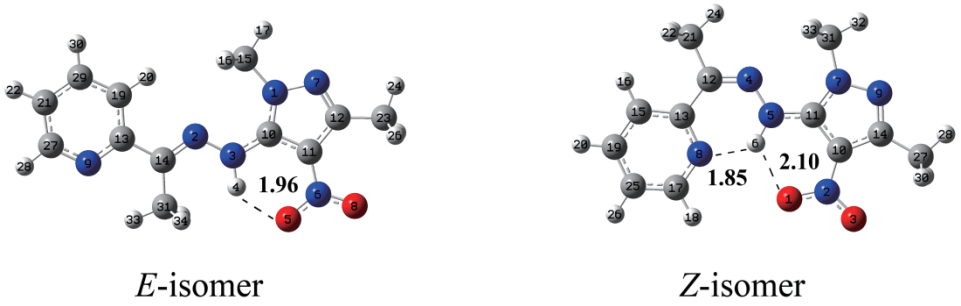

Figure 2. DFT optimized structures of compound **4** at B3LYP/6-311++G** in gas phase; *E*-isomer left and *Z*-isomer right (Numbering of atoms is inside the atoms)

The DFT-optimized structures were in an excellent agreement with the X-ray ones. Figure 3 shows a superimposed representation of the calculated and the experimental structures. The calculated and experimental geometries of the *E*-isomer were nicely overlapped, while for the *Z*-isomer, slight deviations were observed. These deviations involved mostly the position of the hydrogen atoms. Selected calculated parameters are given in Table 4 together with the experimental values for the two rotameric structures (*E*/*Z*). All structural parameters were in accordance with the experimental values. The bond distances showed negligible difference (less than 0.02 Å), while the bond angles showed variations up to 2°. The dihedral angle **C14-N2-N3-C10** in *E*-isomer was slightly larger by 0.9° than that in the crystalline state, while the dihedral angle **C12-N4-N5-C11** in the *Z*-isomer and the crystalline state was the same (180°). The discrepancies are a result of the effect associated to the structural packing constraints on the molecular geometry compared to isolated gas-phase calculated ones.

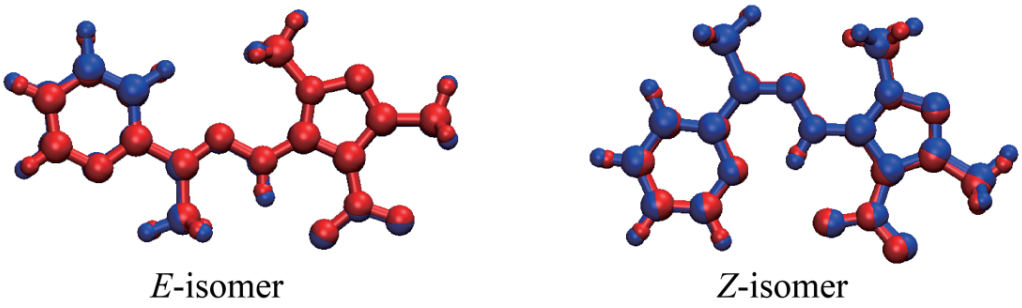

Figure 3. Superimposed structures: experimental *versus* calculated for the two isomers

Table 4. Selected experimental and calculated structural parameters of *E*-isomer and *Z*-isomer; see Figure 2 for the atom numbering. Distances are given in (Å) and angles in (°)

E-isomer			*Z*-isomer		
	Exp.	Calc.		Exp.	Calc.
N2-N3	1.374	1.356	**N4-N5**	1.365	1.349
N1-N7	1.404	1.385	**N7-N9**	1.390	1.382
C10-C11	1.394	1.413	**C10-C11**	1.403	1.414
C13-C14	1.492	1.486	**C12-C13**	1.485	1.480
C14-N2	1.289	1.293	**C13-N8**	1.347	1.348
C11-N6	1.384	1.404	**C11-N5**	1.347	1.361
N6-O5	1.249	1.252	**N2-O1**	1.243	1.245
C14-C13-C19	121.8	121.7	**C12-C13-C15**	121.4	121.3
C10-N1-C15	132.5	130.7	**C11-N7-C31**	132.3	130.9
O5-N6-O8	121.4	123.1	**O1-N2-O3**	122.0	123.4
C14-N2-N3	116.2	117.2	**C12-N4-N5**	119.0	121.3
C14-N2-N3-C10	-177.9	-178.8	**C12-N4-N5-C11**	180.0	180.0

Molecular electrostatic potential (MEP) surface nicely reflects the size, shape, charge density, and reactive groups of the molecule, as well as possible sites of intramolecular and intermolecular interactions. Figure 4 represents the MEP of compound **4** in the two isomeric forms. For both structures, the negative regions are mostly localized over the oxygens of the nitro (NO_2) group, the nitrogen (imine) atom on the pyrazole ring, and the nitrogen atom on the pyridine ring. On the other hand, the positive regions are localized over the hydrogens of pyridine ring and the methyl groups. The green/yellow regions represent the neutral surfaces. The MEP further visualizes the intermolecular/intramolecular interactions sites in both structures, which help in understanding the molecular packing in the solid state.

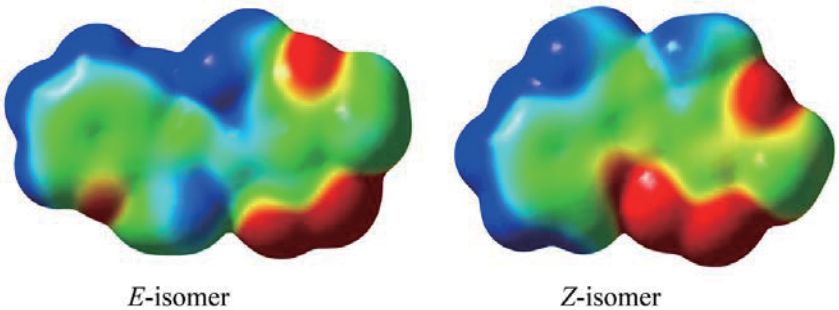

Figure 4. Molecular electrostatic potential of compound **4** in both isomeric forms; red and blue indicates negatively charged and positively charged surfaces, respectively

Indications for the chemical reactivity and kinetic stability of compound **4** can be obtained from the frontier orbital energy gap. A molecule with a small frontier orbital gap is generally more polarizable and is associated with a high chemical reactivity, low kinetic stability and is recognized as soft molecule.[21] The energy of the HOMO is directly related to the ionization potential, while energy of the LUMO is directly related to the electron affinity. The HOMO-LUMO energy gap for compound **4** was calculated for the *E*- and *Z*-isomers as 0.13705 and 0.13365, respectively. The spatial distribution of electron density on HOMO and LUMO orbitals is shown in Figure 5. As shown, the electron density in the HOMO and LUMO is distributed over the molecule. In contrast, the electron density of the HOMO-1 is mainly localized on the pyrazole ring and for the LUMO+2 is concentrated on the pyridine ring.

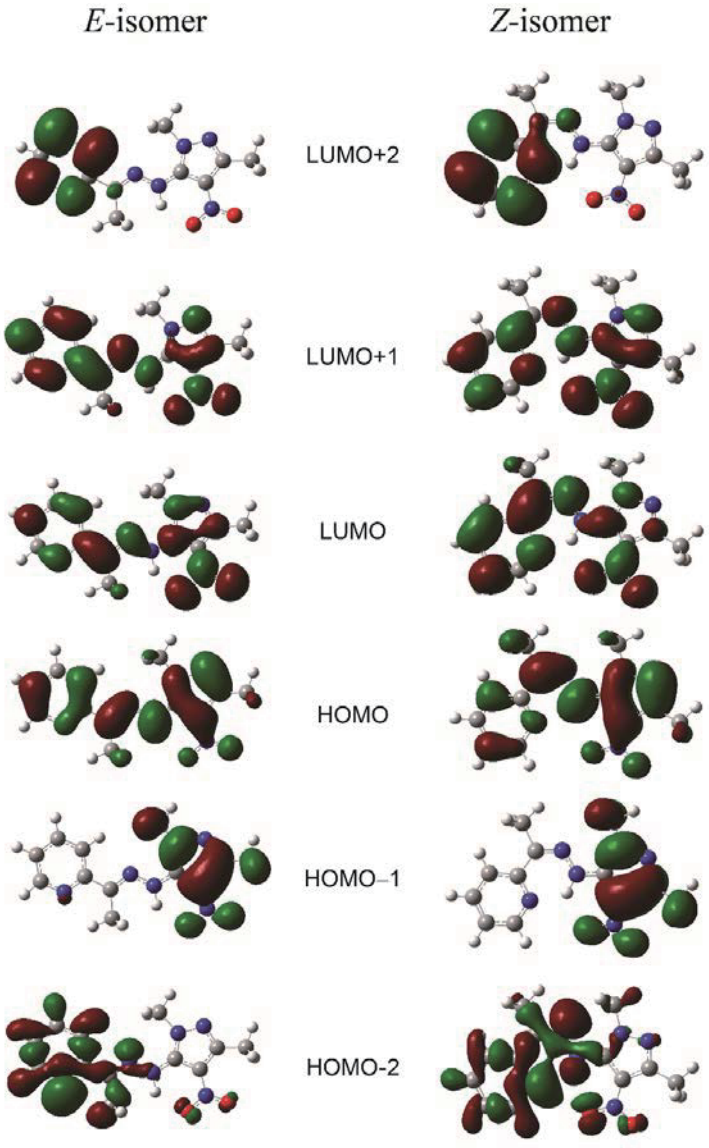

Figure 5. The optimized geometries and the surfaces of the frontier molecular orbitals (HOMOs and LUMOs) of *E*-isomer and *Z*-isomer obtained at the B3LYP/6-311++G** level of theory in gas phase

EXPERIMENTAL

Materials and Instrumentation

Reagent grade chemicals were used as received unless otherwise stated. Melting points (uncorrected) were determined using a Gallenkamp melting point apparatus in one-end open glass capillaries. NMR spectra were recorded on AVANCE-III 400 MHz NanoBay FT-NMR Spectrometer. IR spectra were measured on Brüker Vertex 70 (Germany). Mass spectrum was recorded on Brüker_PC apex-IV Spectrometer. Elemental analyses were done using EA3000 Eurovector (Italy).

5-Hydrazino-1,3-dimethyl-4-nitro-1*H*-pyrazole

The title compound (**2**) was prepared according to the method described previously for 5-chloro-1,3-dimethyl-4-nitropyrazole synthon (**1**).[22]

2-{1-[2-(1,3-Dimethyl-4-nitro-1*H*-pyrazol-5-yl)hydrazono]ethyl}pyridine

To a solution of 2 (0.42 g, 2.4 mmol) in absolute EtOH (40 mL) was added 2-acetylpyridine (0.30 g, 2.4 mmol) in absolute EtOH (10 mL), 1 mL of 10% aqueous HCl. The resulting yellow reaction mixture was stirred for 3 h at reflux temperature and under nitrogen atmosphere. Then the solution was condensed to about 30 mL. Upon cooling at 0 ºC, bright yellow crystalline product was obtained. This was filtered off, dried in a vacuum oven at 50 ºC overnight. The filtrate was concentrated to about 15 mL, whereupon a second crop of product was obtained. The product at this stage is satisfactorily pure for further work. Yield: 0.52 g (90%). A small sample of the product was recrystallized from 1:1 $CHCl_3$-petroleum ether mixed solvent system and the crystals obtained were used for the elemental analyses and the spectroscopic measurements. mp 172-173 ºC. Anal. Calcd for $C_{12}H_{14}N_6O_2$: C, 52.21; H, 5.15; N, 31.97. Found: C, 52.55; H, 5.11; N, 31.66. Mass spectrum shows the molecular ion peak [M+H] at *m*/*z*=275, and [M+Na] at *m*/*z*=297. IR (KBr, cm^{-1}): 3339 (υ(N—H)), 2977 (υ(C—H)), 1668 (υ(C=N)) azomethine, 1582, 1367 (υ(NO_2), 1590 (υ(C=N)) for the pyridine moiety.[23] ^{1}H NMR (400 MHz, DMSO-d_6): δ 2.52 (s, 3H, C<u>H</u>$_3$-C=N), 2.53 (s, 3H, C<u>H</u>$_3$—C)), 4.16 (s, 3H, N—C<u>H</u>$_3$), 7.31 (m, 1H, E), 7.41 (m,1H, Z), 7.74 (m, 1H, E), 7.91 (m, 1H, *Z*), 7.97 (m, 1H, *E*), 7.57 (m, 1H, *Z*), 8.65 (m, 1H, *E*), 8.90 (m, 1H, *E*), 10.23 (br s, 1H, N<u>H</u>-*E*), 15.80 (br s, 1H, N<u>H</u>-*Z*); ^{13}C NMR (100 MHz, DMSO-d_6): δ 11.1 (<u>C</u>H$_3$-C), 14.4 (<u>C</u>H$_3$-C=N), 40.6 (<u>C</u>H$_3$-N), 120.6, 124.7, 137.4, 149.3 (<u>C</u>H of pyridine); 117.8, 142.6, 144.1, 151.7, 154.5 (C-aromatic)

Crystal Structure Determination of 4

Single crystals of **4**, $C_{24}H_{28}N_{12}O_4$ were grown in a 1:1 $CHCl_3$-petroleum ether mixed solvent system. A suitable crystal was selected and mounted on a **Xcalibur**, **Eos** diffractometer. The crystal was kept at 291

K during data collection. Using Olex2[24] the structure was solved with the ShelXT[25] structure solution program using Intrinsic Phasing and refined with the ShelXL[26] refinement package using Least Squares minimization.

Crystal Data for $C_{24}H_{28}N_{12}O_4$ (M =548.58 g/mol): triclinic, space group P-1 (no. 2), a = 10.357(1) Å, b = 11.613(1) Å, c = 13.069(1) Å, α = 67.74(1)°, β = 70.77(1)°, γ = 67.92(1)°, V = 1315.6(3) Å^3, Z = 2, T = 291 K, μ(MoKα) = 0.100 mm^{-1}, *Dcalc* = 1.385 g/cm^3, 11250 reflections measured (5.962° ≤ 2θ ≤ 58.872°), 6078 unique (R_{int} = 0.0296, R_{sigma} = 0.0633) which were used in all calculations. The final R_1 was 0.0543 (I > 2σ(I)) and wR_2 was 0.1510 (all data).

Computational Methods

Quantum chemical calculations were carried out by using Gaussian09 program package.[27] The Becke three parameters hybrid exchange and the Lee–Yang–Parr correlation functional (B3LYP) were used. Ground-state geometry optimization was carried out using 6-311++G** basis set. Frequency calculations were performed for each optimized structure and no imaginary frequency modes were obtained indicating that the structures correspond to true energy minimum.

REFERENCES

1. P. Vicini, F. Zani, P. Cossini, and I. Doytchinova, *Eur. J. Med. Chem.*, 2002, **37**, 553.
2. S. K. Sridhar, S. N. Pandeya, J. B. Stables, and A. Ramesh, *Eur. J. Pharm. Sci.*, 2002, **16**, 129.
3. C. M. Moldovan, O. Oniga, A. Parvu, B. Tiperciuc, P. Varite, A. Pirnau, O. Crisan, M. Bojita, and R. Pop, *Eur. J. Med. Chem.*, 2011, **46**, 526.
4. D. B. Lovejoy and D. R. Richardson, *Blood*, 2002, **100**, 666.
5. P. V. Bernhardt, G. J. Wilson, P. C. Sharpe, D. S. Kalinowski, and D. R. Richardson, *J. Biol. Inorg. Chem.*, 2008, **13**, 107.
6. A. A. R. Despaigne, G. L. Parrilha, J. B. Izidoro, P. R. da Costa, R. G. dos Santos, O. E. Piro, E. E. Castellano, W. R. Rocha, and H. Beraldo, *Eur. J. Med. Chem.*, 2012, **50**, 163.
7. S. Fustero, M. Sanches-Rosello, P. Barrio, and A. Simon-Fuenles, *Chem. Rev.*, 2011, **111**, 6984.
8. A. Ansari, A. Ali, M. Asif, and Shamsuzzaman, *New J. Chem.*, 2017, **41**, 16.
9. H. F. Hoda, M. S. Aladdin, A. I. Mohamed, A. K. Mai, A. S. Rabah, and A. E. May, *Res. Chem. Intermed.*, 2016, **42**, 6881.
10. P. Lv, H. Q. Li, J. Sun, Y. Zhou, and H. Zhu, *Bioorg. Med. Chem.*, 2010, **18**, 4606.
11. A. H. Abadi, A. A. Eissa, and G. S. Hassan, *Chem. Pharm. Bull.*, 2003, **51**, 838.
12. G. M. Nitulescu, C. Draghici, and O. T. Olaru, *Int. J. Mol. Sci.*, 2013, **14**, 21805.
13. H. H. Fahmy, N. M. Khalifa, M. M. F. Ismail, H. M. El-Sahrawy, and E. S. Nossier, *Molecules*, 2016, **21**, 271.

14. J. Liu, M. Zhao, X. Zhang, X. Zhao, and H. Zhu, *Mini-Rev. Med. Chem.*, 2013, **13**, 1957.
15. S. Kumari, S. Paliwal, and R. Chauhan, *Synth. Commun.*, 2014, **44**, 1521.
16. A. S. Abu-Surrah, K. A. Abu Safeih, M. I. Ahmad, M. Y. Abdulla, M. T. Ayoub, A. K. Qaroush, and A. M. Abu-Mahtheieh, *Eur. J. Med. Chem.*, 2010, **45**, 471.
17. R. C. Felicio, E. T. G. Cavalheiro, and E. R. Dockal, *Polyhedron*, 2001, **20**, 261.
18. A. D. Mohamad and M. S. S. Adam, *Chem. Papers*, 2013, **67**, 464.
19. G. E. Iniama, A. Ayi, P. C. Okafor, C. A. Edem, and E. E. O. Duke, *Int. J. Appl. Chem.*, 2014, **10**, 67.
20. S. S. Kandil, A. El-Dissouky, and G. Y. Ali, *J. Coord. Chem.*, 2004, **57**, 105.
21. B. Kosar and C. Albayrak, *Spectrochim. Acta A Mol. Biomol. Spectrosc.*, 2011, **78**, 160.
22. K. A. Abu Safieh, A. M. Abu Mahthieh, M. M. El-Abadelah, M. T. Ayoub, and W. Voelter, *Monatsh. Chem.*, 2007, **138**, 158.
23. R. C. Felicio, E. T. G. Cavalheiro, and E. R. Dockal, *Polyhedron*, 2001, **20**, 261.
24. O. V. Dolomanov, L. J. Bourhis, R. J. Gildea, J. A. K. Howard, and H. Puschmann, *J. Appl. Cryst.*, 2009, **42**, 339.
25. G. M. Sheldrick, *Acta Cryst.*, 2015, **A71**, 3.
26. G. M. Sheldrick, *Acta Cryst.*, 2015, **C71**, 3.
27. M. J. Frisch, G. W. Trucks, H. B. Schlegel, G. E. Scuseria, M. A. Robb, J. R. Cheeseman, G. Scalmani, V. Barone, B. Mennucci, G. A. Petersson, H. Nakatsuji, M. Caricato, X. Li, H. P. Hratchian, A. F. Izmaylov, J. Bloino, G. Zheng, J. L. Sonnenberg, M. Hada, M. Ehara, K. Toyota, R. Fukuda, J. Hasegawa, M. Ishida, T. Nakajima, Y. Honda, O. Kitao, H. Nakai, T. Vreven, J. A. Montgomery, Jr., J. E. Peralta, F. Ogliaro, M. Bearpark, J. J. Heyd, E. Brothers, K. N. Kudin, V. N. Staroverov, T. Keith, R. Kobayashi, J. Normand, K. Raghavachari, A. Rendell, J. C. Burant, S. S. Iyengar, J. Tomasi, M. Cossi, N. Rega, J. M. Millam, M. Klene, J. E. Knox, J. B. Cross, V. Bakken, C. Adamo, J. Jaramillo, R. Gomperts, R. E. Stratmann, O. Yazyev, A. J. Austin, R. Cammi, C. Pomelli, J. W. Ochterski, R. L. Martin, K. Morokuma, V. G. Zakrzewski, G. A. Voth, P. Salvador, J. J. Dannenberg, S. Dapprich, A. D. Daniels, O. Farkas, J. B. Foresman, J. V. Ortiz, J. Cioslowski, and D. J. Fox, Gaussian 09, Revision B.01, Gaussian, Inc., Wallingford C T, 2010.